Deterministic Angle Clustering in Rectangular Buildings Based on Ray-Tracing

Jung-Hyuck Jo, *Member, IEEE*, Mary Ann Ingram, *Senior Member, IEEE*, and Nikil Jayant, *Fellow, IEEE*

***Abstract*—Three-dimensional (3-D) ray-tracing and analysis is used to characterize the path angles in a rectangular building in which all interior walls are parallel or perpendicular to the exterior walls. Path angles are recorded for 500 random transmitter and receiver locations, maintaining constant range throughout a particular building model. The main contribution of this paper is the observation that when all of the path angles from all 500 trials are measured relative to one building wall and collectively analyzed in a signal strength distribution, clustering is clearly apparent. While this angle clustering in the ensemble of channels is not the same as clustering in a single channel trial, it may partially account for the clusters observed in single trials. As a practical matter, these results may impact the use and placement of directional antennas for wireless LANs in buildings of this type.**

***Index Terms*—Indoor radio communication, local area networks, multipath channels, propagation.**

I. Introduction

KNOWLEDGE of the angle associated with a multipath arrival is important because of the increasing use of multiple antenna systems in communications applications. Signals from multiple antennas can be exploited in diversity combining, phased array beam forming, or adaptive array processing algorithms to overcome the effects of multipath. Additionally, multiple antenna systems can enable efficient use of bandwidth by allowing multiple users to simultaneously use the bandwidth, an approach known as space-division multiple access (SDMA) [1]. Finally, a link may reach extremely high spectral efficiency through an architecture of multiple antennas at both ends, popularly described as multiple-input–multiple-output (MIMO) [2]. To predict the performance of these algorithms, stochastic geometric models [4]–[8] and ray-tracing [9]–[13] are often used.

Some stochastic geometric models are "clustered" models. This means that for one or more of their parameters, such as propagation delay, the values are defined in two stages for a given channel trial. The first stage defines a few cluster centers, and the second stage defines the parameters values as relatively small perturbations from the cluster centers. The cluster centers are modeled as random variables. The Saleh and Valenzuela model was the first to define clusters in delay for wireless channels [3]. The model was later extended to include clusters in azimuth angle-of-arrival (AOA) [1]. The AOAs in all geometrical models are typically referenced to the link's line-of-sight (LOS) [4]–[6]. Clustering has been observed in measured channels [1] and is consistent with the IEEE Standard 802.11n model [20]. Clustering degrades the capacity of a MIMO channel [7] and limits the SNR improvement of phased and adaptive arrays [18].

This paper considers clustering in AOA in a certain type of building and with a slightly different definition. The type of building is such that all exterior and interior walls are either perpendicular or parallel to each other, a building type we shall refer to as "normal" in the sequel. The definition of clustering differs from the one above in that the paths of multiple channel trials are superimposed and the AOAs are measured relative to a wall of the building, rather than to the LOS.

By using ray-tracing [9]–[13] and by ignoring cubicle partitions, furniture, windows, occupants and differences between wall, ceiling and floor composition, we show that building-referenced AOAs in normal buildings are clearly clustered. This observation is based on recorded path delays and angles for 500 random transmitter (Tx) and receiver (Rx) pair locations within a simulated normal building assuming the transmitter and receiver are separated by the same distance. As a practical matter, these results may impact the use and placement of directional antennas for wireless LANs in normal buildings.

The remainder of the paper is organized as follows. In Section II, the space-time channel model is described. In Section III, description of simulations and the validation of considered elevation angles of received rays are presented. Then the numerical results of the prediction of indoor wireless channel in space domain are presented in Section IV.

II. Space-Time Channel Model

A. Time of Arrival: TOA

The channel is represented by multiple paths or rays having real positive gains $\{\beta_k\}$, propagation delays $\{\tau_k\}$, and associated phase shifts $\{\theta_k\}$, where k is the path index; in principle, k extends from 0 to ∞. Thus, the complex, low-pass channel impulse response is given by [3]

$$h(t) = \sum_k \beta_k e^{j\theta_k} \delta(t - \tau_k) \tag{1}$$

where $\delta(.)$ is the Dirac delta function.

The parameters β_k, τ_k, and θ_k are randomly time varying functions because of the motion of people and equipment inside and outside of the building. However, the rate of their variations is very slow compared to typical signaling rates. Thus, these parameters can be treated as virtually time-invariant random variables.

Paper approved by R. A. Valenzuela, the Editor for Transmission Systems of the IEEE Communications Society. Manuscript received July 22, 2003; revised March 25, 2004, August 24, 2004, November 23, 2004, and January 5, 2005.

J.-H. Jo is with Samsung Networks, Seoul 135-798, Korea (e-mail: jh2002.jo@samsung.com).

M. A. Ingram and N. Jayant are with the School of Electrical and Computer Engineering, Georgia Institute of Technology, Atlanta, GA 30332-0490 USA.

Digital Object Identifier 10.1109/TCOMM.2005.849979

B. Angle of Arrival: AOA

When no other information is available, it has been typically assumed that the azimuth AOA of multipath components is uniformly distributed in $[0, 2\pi)$ relative to the LOS path between the Tx and the Rx [3]. There are other models that have nonuniform AOA distributions. The Geometrically Based Single Bounce Elliptical Model (GBSBEM) [8] assumes that scatterers are uniformly distributed within an ellipse, where the base station and mobile are the foci of the ellipse. The model was proposed for microcell environments where antenna heights are relatively low, and therefore multipath scattering near the base station is just as likely as multipath scattering near the mobile.

The GBSBEM and similar models assume that the orientations of the reflection surfaces of scatterers are random. However, the orientations of reflection surfaces for a normal building are not random. This is the key observation in this study. As a result, when the AOAs are referenced to the building walls, the AOAs of received rays exhibit clustering.

III. Description of Simulations

A. Ray-Tracing

There are two popular methods that can be employed to calculate the specular reflected and transmitted paths. One is the method of images and the other is often called ray launching. In this paper, the ray launching method is used for ray-tracing simulation. The ray-launching algorithm starts at a transmitter location and sends thousands of test rays in every direction into the numerical environment [9]–[13]. The algorithm searches through the test rays to discover which ones intercept a reception sphere [11]–[13] and then uses these rays to generate profiles of path-signal-strength, path-delays and path-angles, based on geometrical optics. This method is accurate for relatively small areas such as indoor environments where the effect of diffraction is not significant [9]–[12]. Three-dimensional ray-tracing is used in this paper to characterize the path signal strength, delays and angles for four normal buildings.

The ray-tracing simulation parameters are as follows. The maximum number of transmissions and/or reflections is 9, the frequency is 2.4 GHz, the conductivity of the building wall is 0.003 and the relative permittivity of building wall is 4.5. The antenna type modeled for transmitter and receiver is vertically polarized and isotropic. 10351 rays, isotropically spaced on the sphere, are shot from the Tx.

Each set of simulations comprises 500 independent channel trials, where each trial is determined as follows. First, the Tx location is selected at random within a boundary; this boundary corresponds to the external wall of the building for three of the four buildings. For the fourth building, some of locations of Tx are selected outside of the building external wall. The Rx location is then selected at random from the largest arc defined by the distance between Tx and Rx, which is inside the boundary. The profiles of path signal strengths, path delays, and path angles from all 500 trials are collectively analyzed.

The series of simulations is composed of three parts. First, the statistics of the angles of elevation of received rays are analyzed. This part validates that the directional considerations are restricted to the horizontal plane (i.e., azimuth). In the second part, two types of lattice building structure are analyzed. In the third part, the walls of two real buildings are used as the basis for the analysis.

B. Signal Strength

The propagation model in [10] used for calculating the signal strength of the kth ray path (P_k) as

$$P_k = \frac{P_T G_T G_R \lambda^2}{(4\pi r)^2} \prod_i \rho_i \prod_j \tau_j \tag{2}$$

where

P_T	transmitted power [dBm];
G_T, G_R	transmitter and receiver antenna gains [dBi];
λ	wavelength [m];
r	total unfolded path length [m];
ρ, τ	reflected and transmitted power ratios.

The jth trial generates a profile of signal strengths P_k^j, where k is the index of the received ray. The value of k ranges approximately from 100 to 200 depending on the signal strength threshold. Let A_k^j be the azimuth angle in degrees of the kth received ray in the jth trial. The value of each A_k^j is rounded to the nearest degree, resulting in 360 bins of 1-degree width, i.e., $\mathrm{A}_k^j \in \{1, 2, \ldots, 360\}$. Next, all the strengths of all the rays that fall into the ith bin from all 500 trials are summed to give SS_i^{total}. Finally, a moving average is performed on the sequence SS_i^{total} using a 10-degree-wide rectangular window to produce SS_i^{avg}, as follows:

$$SS_i^{\text{avr}} = \frac{1}{10} \sum_{l=-4}^{5} SS_{i+l}^{\text{total}}, \quad i = 1, 2, \ldots, 360 \tag{3}$$

where $i = 360 - i$ if $i < 0$. The ray tracing algorithm spatially samples the electromagnetic (EM) wave as a ray. Therefore, the averaging of received rays is a process of smoothing that makes the ray-tracing results look more like the real field.

C. Elevation Angle

The elevation AOAs are collected using ray-tracing. 171 Rx locations form a 9×19 grid on the fifth floor of the Georgia Centers for Advanced Telecommunications Technology (GCATT) building floor plan, and a Tx is located at the center of the building. Received signal components are neglected if their strength is less than 40 dB below the strongest signal component. Fig. 1 shows a histogram of the elevation angles of the received rays that meet the 40 dB threshold. Each bar height in the graph indicates the percentage of the total rays having that elevation angle. The total number of received rays by 171 Rx locations is 13 688. 53.9% of the rays (7380/13 688) hit the Rx with zero elevation angle; these rays are intentionally eliminated from Fig. 1 so the others can be seen more clearly. 46.1% of the rays (6308/13 688) hit the Rx with a nonzero elevation angle and of these, 70% (4413/6308) of nonzero elevation angles are within the range -20 to 20 degrees. All rays hitting the Rx are within range -45 to 45 degrees. The graph is asymmetric because the height of the Tx and Rx antennas (1.5 m) is slightly less than half the height of the ceiling (3.4 m).

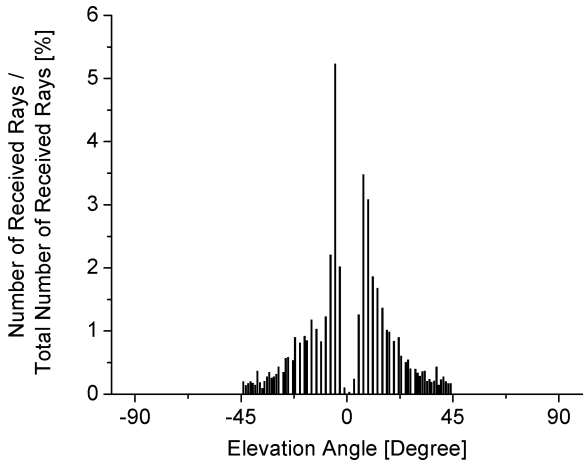

Fig. 1. The graph shows the distribution of the number of received rays of nonzero elevation angle with a signal strength threshold of 40 dB. The number of received rays of zero elevation angles is excluded in this graph, which is 53.9% of total number of received rays.

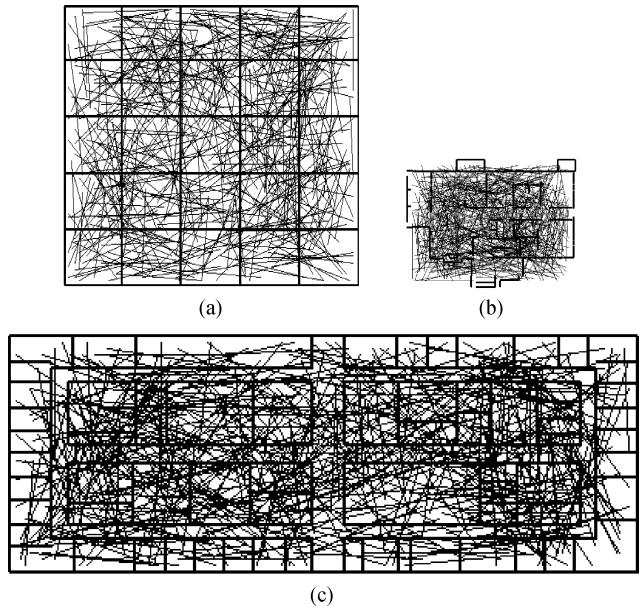

Fig. 2. 500-random Tx–Rx LOS-paths sample locations within a lattice building with (a) sparse-lattice, (b) the first floor of the ResLab, and (c) the fifth floor of the GCATT building. The 500-random Tx–Rx LOS-paths are shown as gray lines. The separation distance between Tx and Rx is (a) 10 m, (b) 7 m, and (c) 15 m. The exterior building wall dimension is (a) 39.2 m by 39.2 m, (b) 17.6 m by 14.6 m, and (c) 72.3 m by 34.2 m, respectively.

The reflection coefficients are very small when the incident EM wave reflects on the floor or the ceiling. In this case, the normal vector to the floor or ceiling is parallel to the polarization of the transmitting antenna. The reflecting surface absorbs most of the EM wave energy when the incident angle is around 20 to 30 degrees, which is the Brewster Angle for the ray tracing parameters mentioned earlier [19]. This is the reason why there are no received rays with elevation angles of around 60 to 70 degrees. From this observation of the elevation angle distributions, directional considerations are restricted to the horizontal plane (i.e., azimuth).

IV. Building-Referenced Angles

The ray-tracing program has been executed with two lattice building structures that were artificially devised for the purpose of analysis, and with two other real building databases. One real building was the Residential Laboratory (ResLab) on the Georgia Tech campus and the other was the fifth floor of the GCATT Building. Therefore, a total of four sets of simulations were performed with four different building databases.

For the lattice building structure, the exterior is modeled as a 39.2 m by 39.2 m square. The ceiling height is 3.5 m. The two different lattice-building structures are distinguished by the number and size of their rooms. The first one, shown in Fig. 2(a), has a distance of 7.84 m between adjacent parallel walls, which is 20% of the exterior wall dimension. The second one, not shown, has a distance of 3.92 m, which is 10% of the exterior wall dimension. Let us call the first one, which has 25 rooms, the *sparse-lattice* model and the second one, which has 100 rooms, the *dense-lattice* model. These are both normal buildings, according to our definition. In real situations, there are rooms and corridors that have a rectangular shape rather than a square, but these generalized building structures represent a typical building shape.

For the first real building database, we used the first floor of the ResLab, which has the external building dimensions of 17.6 m by 14.6 m, and the interior is assumed to have plasterboard and wood walls that extend fully to the 3.3 m-high ceiling. The second real building database we used is the fifth floor of the GCATT Building, which has the external building dimensions of 72.3 m by 34.2 m, and the interior is assumed to have plasterboard and wood walls that extend fully to the 3.4 m-high ceiling. Fig. 2(b) and (c) show the floor plans of the real buildings, respectively.

The distances between the interior walls in the ResLab are longer than the distances between the interior walls in the GCATT Building, as shown in Fig. 2(b) and (c). In other words, the sparse-lattice model is more like the ResLab Building and the dense-lattice model is more like the GCATT Building.

A. Lattice Building Structures

The solid line in Fig. 3 shows the clustering patterns observed with the Tx–Rx range of 20 m within the sparse-lattice building. The ith bin value of signal strength, SS_i^{avr}, is normalized to the strongest among the values of 360 bins. The mean angles of the clusters are 45, 135, 225 and 315 degrees, regardless of the Tx–Rx ranges considered, and regardless of the type of lattice (sparse or dense). Furthermore, the signal strength differences between peak and bottom are about 2–4 dB.

Let us define the ratio of the Tx–Rx range to the distance between adjacent parallel walls within a building as d. In other words, d is the maximum number of walls the LOS passes through to reach the Rx. Then, the values of d are 1.91, and 3.19 for Tx–Rx ranges of 15 m and 25 m, respectively, for the sparse lattice building, and 1.28 and 3.06 for the Tx–Rx ranges of 5 m and 12 m, respectively, for the dense lattice building. We found (results not shown because of space limitations) that only if the d value ranges from 1.2 to 3.2, the clustering of signal strengths is apparent with mean angles of 45, 135, 225, and 315 degrees regardless of the actual distance between Tx

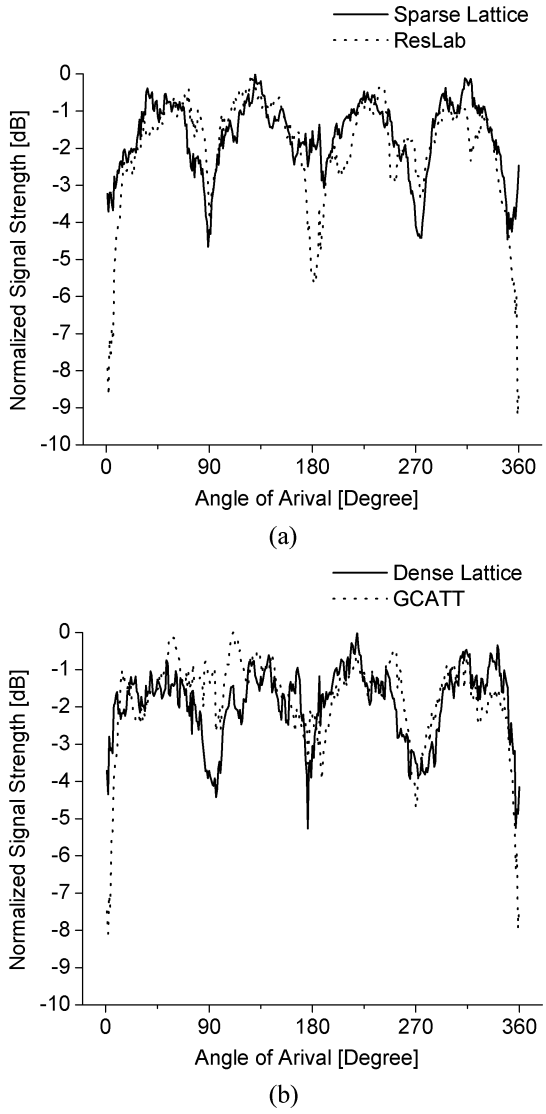

Fig. 3. Signal strength distribution: AOAs are referenced to the exterior building wall. The signal strength is normalized. The Tx–Rx ranges are (a) 10 m in sparse-lattice and the ResLab, and (b) 5 m in dense-lattice and 10 m in the GCATT building.

and Rx. Therefore, we can say that the ratio of a side-length of a square room and the distance between Tx and Rx affects the clustering patterns. If the d ranges out of 1.2 to 3.2, the received signal strengths' distributions are almost uniform over 0 to 360 degrees in azimuth.

B. Real Building Structures

The dotted and dashed lines in Fig. 3 show the clustering patterns of received signal strength, SS_i^{avr}, observed with the Tx–Rx range of 10 m within the first floor of the ResLab and the fifth floor of the GCATT Building, respectively. The mean angles of clusters are also same as the lattice building model cases.

C. Mathematical Model of Angle Clustering

The clustering pattern of signal strength distributions in angles referenced to exterior building wall shows a sinusoidal periodicity as in Fig. 3. To find an analytical model for the clustering

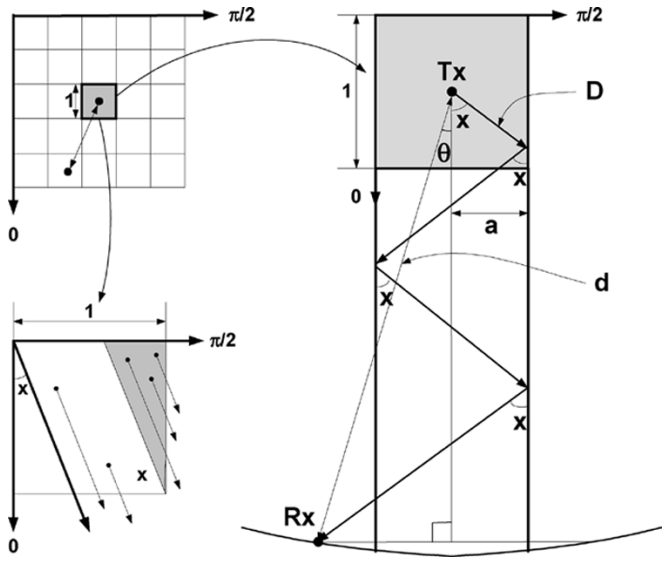

Fig. 4. The upper left shows a lattice building structure, and the lower left and the right both represent one magnified unit square in a lattice building structure. The lower left illustrates the calculation of a probability that a launched ray hits a vertical wall, $f_Y(x)$, which is the shaded area. The right illustrates a reflection mechanism within a lattice building structure.

pattern in a normal building, we assume the lattice structure as shown in Fig. 2(a) and consider only one column of rooms.

Let a "vertical wall" mean parallel to the external reference wall and let all other wall be "horizontal." Let us find the probability that a ray launched at a particular angle x relative to the external wall hits the vertical (or horizontal) interior lattice wall when the launching point (Tx position) is chosen randomly within a lattice square as in Fig. 4. Either a horizontal or a vertical wall could be considered because of the symmetry of the building structure. Then, the probability of the launched rays hitting vertical wall, Y, is the ratio of the shaded area to the area of the square in Fig. 4. This probability Y is a function of launching angle x in degrees and is given by

$$Y = \begin{cases} \frac{1}{2}\tan x, & 0 < x \le 45^\circ \\ 1 - \frac{1}{2}\tan\left(\frac{\pi}{2} - x\right), & 45^\circ < x \le 90^\circ \\ 1 - \frac{1}{2}\tan\left(x - \frac{\pi}{2}\right), & 90^\circ < x \le 135^\circ \\ \frac{1}{2}\tan(\pi - x), & 135^\circ < x \le 180^\circ \end{cases} \tag{4}$$

for $0 < \mathrm{x} < 180$ degrees. We can find the other half of the Y easily, for $180 < \mathrm{x} \le 360$ degrees, because of the symmetry of the building structure. The plot for $Y = f_Y(x)$, is shown in Fig. 5 as a solid line.

To simplify our analysis, we shall neglect these paths that do not first reflect on the wall in the originating room. Then, we can get an expression for the expected value of the signal strength, $S(x)$, as a function of x. $S(x)$ is a function of the initial strength α, the probability that a launched ray hits a vertical wall $f_Y(x)$, the reflection coefficient $R(\varepsilon_r, \sigma, f, x)$, the number of reflections $k(d, x)$, and path loss $PL(D_p, f)$, and is given by

$$S(x) = \alpha \cdot f_Y(x) \cdot R(\varepsilon_r, \sigma, f, x)^{k(d,x)} \cdot PL(D_p, f) \tag{5}$$

$$PL(D_p, f) = \frac{G_T \cdot G_R \cdot \left(\frac{c}{f}\right)^2}{(4\pi \cdot D_p)^2} \tag{6}$$

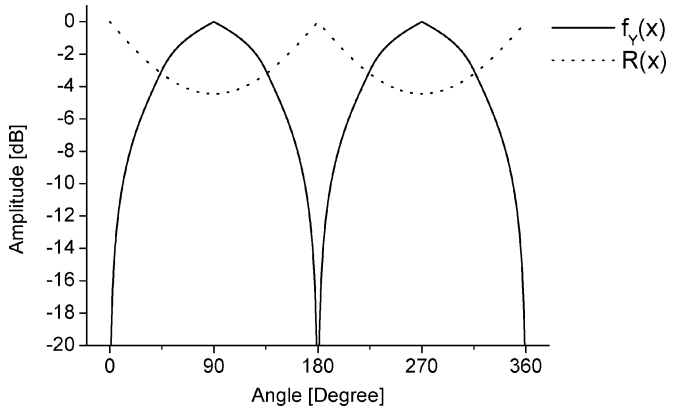

Fig. 5. The probability that a launched ray hits a vertical wall, $f_Y(x)$ as a solid line and the plot of reflection coefficient, $R(x)$ with perpendicular polarization as a dotted line.

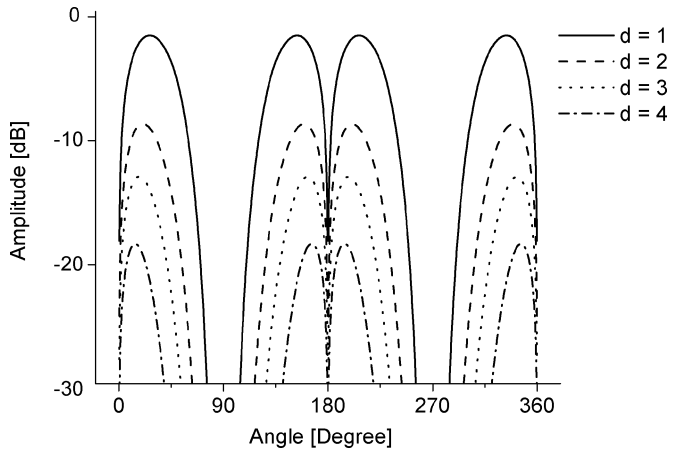

Fig. 6. The signal strength distributions, $S(x)$ in angles referenced to the exterior building wall.

where ε_r is a relative permittivity, σ is a conductivity, f is a frequency of the ray, c is the velocity of light, d is a direct path length between Tx and Rx, D_p is an unfolded propagation path length of a ray from Tx to Rx, G_T and G_R are Tx and Rx antenna gains respectively, and k is the number of reflections as a function of d and x. Both d and D_p are normalized by the distance between adjacent parallel walls.

The derivation of k is as follows. In Fig. 4, Rx can move on an arc centered by Tx because one of the conditions for the simulation is maintaining a direct path length d between Tx and Rx. In this analysis, let us assume the angle, θ, of the LOS path between Tx and Rx referenced to the building wall ranges from -45 to 45 degrees. Another assumption is that the angle, x, of the ray emitting from Tx ranges from 0 to 90 degrees. Then, D_p and d are related by

$$D_p = \frac{\cos x}{\cos\theta} \cdot d. \tag{7}$$

In Fig. 4, a is the distance between the Tx and a vertical wall. Then, D_p and a are related by, for two cases

1) *the location of Rx is inside the column*

$$D_p = \sum_{i=1}^{k} \frac{1}{\sin x} + \frac{d \cdot \sin\theta + 2a - 1}{\sin x}. \tag{8a}$$

2) *the location of Rx is outside the column*

$$D_p = \sum_{i=1}^{k-1} \frac{1}{\sin x} + \frac{-d \cdot \sin\theta + 1}{\sin x}. \tag{8b}$$

By substituting D_p in (8) into (7), we can derive an equation for k as

1) *the location of Rx is inside the column*

$$k = d \cdot \tan x \cdot \cos\theta - d \cdot \sin\theta - 2a + 1. \tag{9a}$$

2) *the location of Rx is outside the column*

$$k = d \cdot \tan x \cdot \cos\theta + d \cdot \sin\theta \tag{9b}$$

where $0 < a < 1$ and $0 < x < 90$ degrees. We may extend the definition of k to be a function for all x by using the symmetry of the building structure:

1) *the location of Rx is inside the column*

$$k(d,x) = \lceil d \cdot \cos\theta \cdot |\tan x| - d \cdot \sin\theta - 2a + 1 \rceil. \tag{10a}$$

2) *the location of Rx is outside the column*

$$k(d,x) = \lceil d \cdot \cos\theta \cdot |\tan x| + d \cdot \sin\theta \rceil \tag{10b}$$

where $0 < a < 1$ and $0 < x < 360$ degrees.

The wall reflection coefficient assuming a vertically polarized wave is given by

$$R_\perp = \frac{\sin x - \sqrt{\varepsilon - \cos^2 x}}{\sin x + \sqrt{\varepsilon - \cos^2 x}} \tag{11}$$

where $\varepsilon = \varepsilon_r - j60 \cdot \sigma \cdot c/f$. x is an incident angle of the ray.

Fig. 5 shows the plots of $f_Y(x)$ and the reflection coefficient R as a function of x. Fig. 6 shows the plots of the signal strength distribution, $S(x)$, for $d = 1$, 2, 3, and 4. We can see the similarities between the plots of $S(x)$ in Fig. 6 and the clustering patterns as a result of simulation in Fig. 3. The mean angles of the clusters are close to 45, 135, 225, and 315 degrees. Intuitively, if a ray is launched from the Tx with an angle of around 0 (360) or 180 degrees, the ray hits the vertical wall with a relatively low probability, but the reflection coefficient is relatively large. At these angles, the low probability causes local minima in the signal strength distribution. On the other hand, if a ray is launched from Tx with an angle of around 90 or 270 degrees, the ray has a relatively high probability to hit the vertical wall while the reflection coefficient is weakest. Therefore, at these angles, it is the reflection coefficient that causes the local minima. Note that the effect of the reflection coefficient is enhanced by its exponent k in (5), which increases with distance d. This explains why heights and locations of the peaks in $S(x)$ change slightly with distance d.

V. Conclusion

In this paper, the AOA of received rays in a rectangular building were intensively studied. The statistics of azimuth AOA of received rays referenced to the exterior building wall were presented with a lattice-building database and with a real building database. Multiple clusters were clearly observed in the azimuth AOAs of the ensemble of received rays. A mathematical model of the angle clustering phenomenon of the received signal strength within a rectangular shaped building was given.

The results of this study suggest that antennas with nonadaptive patterns that match to the clusters may enhance the performance of wireless LAN in rectangular buildings.

ACKNOWLEDGMENT

The authors wish to thank the anonymous reviewers for their insightful comments and helpful critiques of the manuscript.

REFERENCES

[1] R. H. Roy, "Spatial division multiple access technology and its application to wireless communication systems," in *Proc. IEEE Vehicular Technology Conf.*, vol. 2, May 1997, pp. 730–734.
[2] S. Catreux, L. J. Greenstein, and V. Erceg, "Some results and insights on the performance gains of MIMO systems," *IEEE J. Sel. Areas Commun.*, vol. 21, no. 5, pp. 839–847, Jun. 2003.
[3] A. M. Saleh and R. A. Valenzuela, "A statistical model for indoor multipath propagation," *IEEE J. Sel. Areas Commun.*, vol. SAC-5, no. 2, pp. 128–137, Feb. 1987.
[4] Q. Spencer *et al.*, "Modeling the statistical time and angle of arrival characteristics of an indoor multipath channel," *IEEE J. Sel. Areas Commun.*, vol. 18, no. 3, pp. 347–360, Mar. 2000.
[5] O. Norklit and J. B. Andersen, "Mobile radio environment and adaptive arrays," in *Proc. 5th IEEE Int. Symp. Personal, Indoor and Mobile Radio Communications*, vol. 2, 1994, pp. 725–728.
[6] O. Norklit *et al.*, "The angular aspect of wide-band modeling and measurements," in *Proc. 4th IEEE Int. Symp. Spread Spectrum Techniques and Applications*, vol. 1, 1996, pp. 73–78.
[7] K.-H. Li and M. A. Ingram, "Impact of clustering in statistical indoor propagation models on link capacity," *IEEE Trans. Commun.*, vol. 50, no. 4, pp. 521–523, Apr. 2002.
[8] J. C. Liberti and T. S. Rappaport, "A geometrically based model for line of sight multipath radio channels," in *Proc. IEEE Vehicular Technology Conf.*, Apr. 1996, pp. 844–848.
[9] R. A. Valenzuela, "A ray tracing approach to predicting indoor wireless transmission," in *Proc. IEEE Vehicular Technology Conf.*, May 1993, pp. 214–218.
[10] R. A. Valenzuela, O. Landron, and D. L. Jacobs, "Estimating local mean signal strength of indoor multipath propagation," *IEEE Trans. Veh. Technol.*, vol. 46, no. 1, pp. 203–212, Feb. 1997.
[11] S. Y. Seidel and T. S. Rappaport, "Site-specific propagation prediction for wireless in-building communication system design," *IEEE Trans. Veh. Technol.*, vol. 43, no. 4, pp. 879–891, Nov. 1994.
[12] T. S. Rappaport, G. D. Durgin, and N. Patwari, "An advanced 3-D ray launching method for wireless propagation prediction," in *Proc. IEEE Vehicular Technology Conf.*, vol. 2, May 1997, pp. 785–789.
[13] G. D. Durgin, N. Patwari, and T. S. Rappaport, "Improved 3-D ray launching method for wireless propagation prediction," *Electron. Lett.*, vol. 33, no. 16, pp. 1412–1413, Jul. 1997.
[14] M. Lu, T. Lo, and J. Litva, "A physical spatio-temporal model of multipath propagation channel," in *Proc. IEEE Vehicular Technology Conf.*, 1997, pp. 810–814.
[15] R. B. Ertel and J. H. Reed, "Angle and time of arrival statistics for circular and elliptical scattering models," *IEEE J. Sel. Areas Commun.*, vol. 17, no. 11, pp. 1829–1840, Nov. 1999.
[16] *Microwave Mobile Communications*, J. William and C. Jakes, Eds., Wiley, New York, 1974.
[17] T. Lo and J. Litva, "Angles of arrival of indoor mutipath," *Electron. Lett.*, vol. 28, no. 18, pp. 1687–1689, Aug. 1992.
[18] J. H. Winters, "The range increase of adaptive versus phased arrays in mobile radio systems," *IEEE Trans. Veh. Technol.*, vol. 48, no. 2, pp. 353–362, Mar. 1999.
[19] J. D. Kraus, *Electromagnetics*. New York: McGraw-Hill, 1991.
[20] *TGn Indoor MIMO WLAN Channel Models*, IEEE 802.11–03–161r2.

Jung-Hyuck Jo (S'98–M'02) received the B.S. and M.S. degrees in electronics engineering from Korea University, Seoul, Korea, in 1994 and 1996, respectively, and the Ph.D. degree in electrical and computer engineering from the Georgia Institute of Technology (Georgia Tech), Atlanta, in 2003.

Since 2003 he has been with Samsung Networks, where he is leading the internet business development group. His research interests are in the fields of broadband wireline/wireless/mobile communications and security of networks.

Mary Ann Ingram (M'85–SM'03) received the B.E.E. and Ph.D. degrees from the Georgia Institute of Technology (Georgia Tech), Atlanta, in 1983 and 1989, respectively.

From 1983 to 1986, she was a Research Engineer with the Georgia Tech Research Institute, Atlanta, performing studies on radar electronic countermeasure (ECM) systems. In 1986, she became a Graduate Research Assistant with the School of Electrical and Computer Engineering at Georgia Tech, where in 1989, she became a Faculty Member and is currently Professor. Her early research areas were optical communications and radar systems. In 1997, she established the Smart Antenna Research Laboratory (SARL), which emphasizes the application of multiple antennas to wireless communication systems. The SARL performs system analysis and design, channel measurement, and prototyping relating to a wide range of wireless applications, including wireless local area network (WLAN) and satellite communications, with focus on the lower layers of communication networks.

Nikil Jayant (M'69–SM'77–F'82) received the Ph.D. degree in electrical communication engineering from the Indian Institute of Science, Bangalore, India. As part of this doctoral program, he was a Research Associate at Stanford University, Stanford, CA, for one year prior to joining Bell Labs, Murray Hill, NJ, in 1968.

He joined the faculty of the Electrical and Computer Engineering Department, Georgia Institute of Technology (Georgia Tech), Atlanta, in July 1998, as a Georgia Research Alliance Eminent Scholar, as the John Pippin Chair in Wireless Systems, and as the Director of the Georgia Tech Wireless Institute. In April 1999, he created and became the first Director of the Georgia Tech Broadband Institute, with cross-campus responsibilities in research and industry partnership in broad-band access, lifestyle computing, and ubiquitous multimedia. In October 2000, he was named Executive Director of the Georgia Centers for Advanced Telecommunications Technology (GCATT). In 2004, he was named Director of Strategic Partnerships for Georgia Institute of Technology, with initial focus on industry partnerships in communications, computing and content. Earlier in his career at Bell Laboratories, Dr. Jayant created and managed the Signal Processing Research Department, the Advanced Audio Technology Department and the Multimedia Communications Research Laboratory. He also initiated several new ventures for AT&T and Lucent Technologies, including businesses in Internet Multimedia, Wireless Communications and Digital Audio Broadcasting. Recently, he served as the Chairperson of the National Academies Committee on Broadband Last Mile Technologies. He co-founded EGTechnology, an Atlanta-based startup company engaged in creating broad-band platforms, with initial focus on software for advanced television. He is also the Founder and President of MediaFlow, a consulting company. He has served on the Advisory Board of NTT-DoCoMo (USA), and is currently a Scientific Advisor to the Singapore Institute for Infocomm Research. His personal research has been in the field of digital coding and transmission of information signals. He has published 130 papers, authored or co-authored five books, and is also the author of 35 patents.

Dr. Jayant has received several honors, including the IEEE Browder J. Thompson Memorial Prize Award (for the best IEEE publications by an author under thirty years of age, 1974), the IEEE Donald G. Find Prize Paper Award (for the best tutorial in an IEEE publication, 1995), and the Lucent Patent Recognition Award (1997). In 1998, he was inducted into the New Jersey Inventors Hall of Fame. He was the Founding Editor-in-Chief of the IEEE *ASSP Magazine*. He is a Fellow of the IEEE, a recipient of the IEEE Third Millennium Medal, and a member of the National Academy of Engineering.